



ELSEVIER

Contents lists available at ScienceDirect

## Theoretical Population Biology

journal homepage: [www.elsevier.com/locate/tpb](http://www.elsevier.com/locate/tpb)

## Stabilization of metapopulation cycles: Toward a classification scheme

Refael Abta<sup>a</sup>, Marcelo Schiffer<sup>b</sup>, Avishag Ben-Ishay<sup>a</sup>, Nadav M. Shnerb<sup>a,\*</sup><sup>a</sup> Department of Physics, Bar-Ilan University, Ramat-Gan 52900, Israel<sup>b</sup> Department of Physics, Ariel University Center of Samaria, Ariel 44837, Israel

## ARTICLE INFO

## Article history:

Received 8 October 2007

Available online xxxx

## Keywords:

Coexistence

Competition

Noise

Spatial models

Predation

Diversity

Dispersal

Desynchronization

## ABSTRACT

The stability of population oscillations in ecological systems is considered. Experiments suggest that in many cases the single patch dynamics of predator–prey or host–parasite systems is extinction prone, and stability is achieved only when the spatial structure of the population is expressed via desynchronization between patches. A few mechanisms have been suggested so far to explain the inability of dispersal to synchronize the system. Here we compare a recently discovered mechanism, based on the dependence of the angular velocity on the oscillation amplitude, with other, already known conditions for desynchronization. Using a toy model composed of diffusively coupled oscillators we suggest a classification scheme for stability mechanisms, a scheme that allows for either *a priori* (based on the system parameters) or *a posteriori* (based on local measurements) identification of the dominant process that yields desynchronization.

© 2008 Elsevier Inc. All rights reserved.

## 1. Introduction

Victim–exploiter systems are very common in nature, and their sustainability is a long-standing puzzle, first pointed out by ancient day naturalists such as Herodotus and Cicero (Cuddington, 2001). Although in nature such a system is usually embedded in an entire food web, the understanding of that web’s basic constituent, namely, the two species (predator–prey or host–parasite) system, is a crucial step toward the explanation of the “balance of nature” in general. An “isolated” victim–exploiter system may be achieved either experimentally (where the only important parameters in a given setup are the densities of the two species involved) or theoretically, where the corresponding process is presented and (analytically or numerically) solved.

The mathematical modeling of the two-species system is usually based on Lotka–Volterra (LV) predator–prey equations (Lotka, 1920; Volterra, 1931; Murray, 1993) or the Nicholson–Bailey (NB) map for host–parasite interaction (Nicholson and Bailey, 1935). Lotka and Volterra describe a predator–prey interaction (overlapping generations) by the continuous differential equations,

$$\begin{aligned} \frac{da}{dt} &= -\mu a + \lambda_1 ab \\ \frac{db}{dt} &= \sigma b - \lambda_2 ab, \end{aligned} \quad (1)$$

where  $a$  is the predator density (decaying exponentially with rate  $\mu$  in the absence of prey),  $b$  is the prey density (growing exponentially with rate  $\sigma$  in the absence of predators), and  $\lambda_1$  and  $\lambda_2$  are the relative increase (decrease) of the predator (prey) populations due to the interaction between species, correspondingly.

The Nicholson and Bailey map is considered a fundamental model for host–parasite systems, as it assumes non-overlapping generations. The host density  $H$  and the parasite density  $P$  at the  $t + 1$  generation are determined by

$$\begin{aligned} H_{t+1} &= \sigma H_t e^{-\lambda P_t}, \\ P_{t+1} &= c H_t (1 - e^{-\lambda P_t}), \end{aligned} \quad (2)$$

where  $\sigma > 1$  is the growth factor of the host in the absence of a parasite.

Both the NB and the LV equations share some important features:

- **Neglect of spatial structure:** the models assume that the chance for predation or for infection is constant for any exploiter–victim pair of animals in the system and is independent of their spatial location. This may be true if the size of the system is “small”, given the migration rate of the individuals, or if dispersal induces some sort of coherence in the system, such that any individual sees the same environment.
- **Determinism:** The state of the system at  $t$  dictates its state in the next time step. Such a description ignores the effect of noise, existing in any ecological system and experimental setup. Describing a stochastic process by deterministic dynamics

\* Corresponding author.

E-mail address: [shnerbn@mail.biu.ac.il](mailto:shnerbn@mail.biu.ac.il) (N.M. Shnerb).

is, in the best case, an approximation; the quality of this approximation should be considered explicitly for any system of that type (Gardiner, 2004).

- **Instability:** LV and NB both admit a coexistence fixed point; however, this point is not stable. The LV equations admit a conserved quantity  $K = \lambda_1 b + \lambda_2 a - \mu \ln(a) - \sigma \ln(b)$ . This implies that the fixed point is marginally stable: once the system is perturbed (say, by noise) and hits a value of  $K$ , it will stay on that trajectory forever. Consequently, any type of noise will drive the system randomly in the  $K$  space until one of the species goes extinct (estimation of the extinction time under such conditions is known as the *first passage problem*; see Redner (2001)). The NB system is even worse: its fixed point is unstable and the trajectory approaches extinction very quickly. Thus, both the LV and the NB systems are extinction prone in the absence of spatial-structure induced effects.

Of course, there are lots of modifications of the naive LV and NB mathematical descriptions, taking into account many realistic factors like finite carrying capacity, time delay, Allee effect, age structured populations, density dependent predation, etc. Some of these generalized models are not extinction prone, admitting stable manifolds such as a stable fixed point, limit cycle or (for systems with more than two components) strange attractor. However, since the work of Gause (1934) through the classic experiments of Pimentel et al. (1963), Luckinbill (1974) and Huffaker (1958), it was known that small sized predator prey (or hosts and parasites) systems reach extinction in experimental time scales. In the last decade, the experiments of Holyoak and Lawler (1996), Kerr et al. (2002, 2006), Kirkup and Riley (2004) and Ellner et al. (2001) demonstrate the fact that systems go extinct rapidly in the well-mixed limit while persisting way above the experimental time (up to hundreds of generations) when the population is spatially segregated. It follows that in many cases, and perhaps even generically, victim–exploiter systems are unstable in the well-mixed limit, and acquire their stability only due to the spatial structure.

These findings provide support for Nicholson's (1933) old proposal regarding migration induced stabilization, i.e., that *desynchronization* between weakly coupled spatial patches, together with the effect of migration, stabilizes the global populations. To understand the mechanism, let us imagine a metapopulation on two patches, where within each patch the population oscillations are governed by, say, Lotka–Volterra dynamics where constant diffusion (i.e., density independent per capita migration rate) exists between these two patches. Clearly, as emphasized in Fig. 1, if the oscillations on these two patches desynchronized, e.g., if one of the patches is densely populated while the other is, at the same time, diluted, migration between patches pushes the whole system inward toward the coexistence fixed point, yielding sustained oscillations. However, one should bear in mind that dispersal is a double-edged sword, as it tends to reduce population gradients and induce synchronization. The litmus test for Nicholson's proposal is thus as follows: is the diffusion among patches weak enough to allow noise induced desynchronization, but at the same time strong enough to stabilize desynchronized patches? If this is to be the case, the desynchronization–diffusion stabilization mechanism may work.

The conditions for desynchronization in diffusively coupled patches have been examined in many studies, and the main results, summarized in a recent review article (Briggs and Hoopes, 2004), are as follows:

- For any deterministic network of  $N$  identical patches, if the migration between patches is symmetric or almost symmetric (i.e., the diffusion of the prey and the predator are, more or less, the same), the dispersal between patches yields

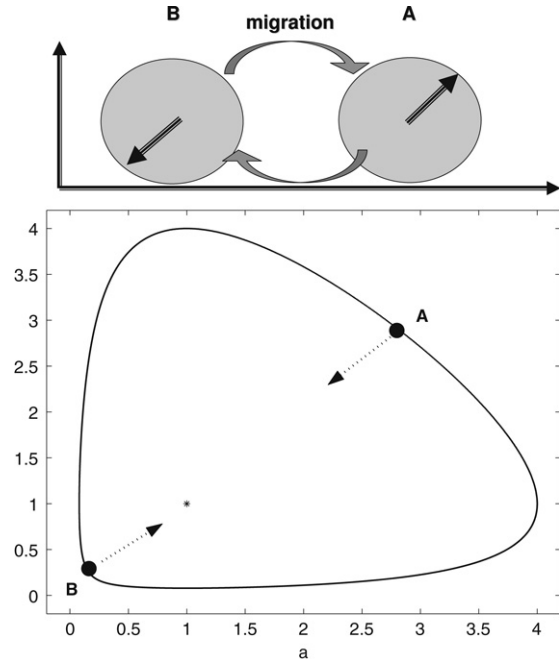


**Fig. 1.** Population oscillation on two spatial patches coupled by migration. If both patches desynchronize, one may find one of them (A) in the dense population state and the other one (B) in the diluted phase. Diffusion tends to decrease population gradients, and hence the whole system flows toward the coexistence fixed point, represented in the lower panel by an asterisk.

synchronization. Accordingly, the homogenous manifold is stable – small spatial fluctuations are smeared out by migration – and the stability properties of the fixed point are identical with that of the non-spatial model (Crowley, 1981; Allen, 1975; Reeve, 1990). Thus, the effect of migration alone does not resolve the instability problem; if the well-mixed system is extinction prone, so is its spatial analogue. An exception is the result of Adler (Adler, 1993; Reeve, 1988; Taylor, 1998) for the discrete time NB model, where some initial conditions seem to converge, or almost converge, to a periodic orbit for some range of migration values. In this paper we limit ourselves to continuous time models, and the relation of Adler's result to the presented stabilization mechanisms is briefly discussed below.

- The system may become desynchronized in the presence of spatial heterogeneity, e.g., where the reaction parameters vary on different spatial patches (Murdoch and Oaten, 1975). In that case, the intrinsic dynamic at any localized patch takes place on different time scales for the same concentrations, so diffusion fails to synchronize different patches. This mechanism may be generalized to include not only “quenched” heterogeneity but also environmental stochasticity, i.e., where the reaction parameters are subject to spatio-temporal fluctuations (Reeve, 1988, 1990).
- **Diffusion induced** instability may occur if the migration rate of the predator is much smaller than that of the prey, particularly if the prey migration rate is zero (Jansen, 1995; Abta and Shnerb, 2007b).

Recently, we presented another solution to this puzzle (Abta et al., 2007a). The solution is, mathematically speaking, more generic, as it depends only on demographic stochasticity (which must exist in both natural and experiment systems) and is independent of external assumptions, such as space–time fluctuations or variance in migration patterns. We have shown that the basic ingredient that leads to desynchronization is the dependence of the angular velocity of the orbit on its amplitude, a generic feature of

nonlinear systems. The interaction between nonlinearity and noise stabilizes the otherwise unstable fixed point.

In order to understand the observed stability of a spatially extended victim–exploiter system, one should consider a few possible mechanisms. Typically, the system admits both demographic and environmental stochasticity, the migration rates are at least slightly different and the exact mathematical description of the nonlinear dynamics is unknown. In this paper we provide an initial sketch of a classification scheme based on a toy model first presented in (Abta et al., 2007a). It turns out that all the suggested mechanisms for desynchronization induced stability may be described by that simple toy model, and that only 3–4 parameters are needed for an *a priori* estimate of the relative importance of certain mechanisms. Moreover, even when a sound estimate of these parameters is impossible, the insight gained from the toy model allows one to identify *a posteriori* the dominant mechanism using local measurements or observations.

Throughout this paper, we limit ourselves to the continuous time, two-patch case; more complicated situations (and the important question of synchronization length given the nonlinear dynamics and the migration rate) will be addressed elsewhere. In the next section we describe the toy model, then use it to analyze and explain the stabilizing mechanism suggested thus far. *A priori* and *a posteriori* means of identification are suggested in each case. While far from being complete, we believe that the scheme presented here may serve as a basic tool for the analysis of desynchronization on spatial domains, as will be discussed in the last section.

## 2. Toy model: Coupled oscillators

Let us assume that the well-mixed dynamics of an ecological system is unstable, i.e., that the amplitude of oscillations around the coexistence fixed point grows in time until extinction. We assume further that the system acquires its stability due to spatial structure, and limit ourself to the case of two coupled patches.

A simple, and quite generic description of the deterministic nonlinear dynamics around the coexistence fixed point is given by a toy model that deals with the phase space behavior of *diffusively* coupled oscillators (the origin of that toy model corresponds to the coexistence point of the LV/NB models), where the angular velocity depends on the phase space location:

$$\begin{aligned} \frac{dx_1}{dt} &= \omega(x_1, y_1)y_1 + D_1(x_2 - x_1) + \alpha x_1 \\ \frac{dy_1}{dt} &= -\omega(x_1, y_1)x_1 + D_2(y_2 - y_1) + \alpha x_2 \\ \frac{dx_2}{dt} &= \omega(x_2, y_2)y_2 + D_1(x_1 - x_2) + \alpha y_1 \\ \frac{dy_2}{dt} &= -\omega(x_2, y_2)x_2 + D_2(y_1 - y_2) + \alpha y_2. \end{aligned} \quad (3)$$

Here  $\alpha$  stands for the instability, and it corresponds to the Lyapunov exponent of the (continuous time analogue of the) Nicholson–Bailey system; the marginally stable (Lotka–Volterra) case corresponds to  $\alpha = 0$ . In the marginal case the radius of oscillations  $r$  is conserved on the homogenous manifold, but the angular velocity may depend on either  $r$ , the radius of oscillations, or  $\theta$ , the azimuthal angle. We are going to show that the essence of all the mechanisms that yield desynchronization is captured by this model. The only difference between them is related to the function  $\omega(x, y)$ : if  $\omega$  is fixed, the system synchronizes and the oscillation amplitude grows unboundedly. When  $\omega$  differs between patches for some reason, desynchronization occurs, and the oscillation stabilizes.

The dependence of the angular velocity  $\omega$  on the phase space coordinates is quite complicated for the NB and LV models. Things become much simpler when the dependence of  $\omega$  is either on the distance from the coexistence fixed point  $r$  or on the azimuthal angle  $\theta$ . In particular, if  $\omega$  is  $\theta$  independent, the system of Eq. (3)

becomes simpler in polar coordinates. Defining  $r_i \equiv \sqrt{x_i^2 + y_i^2}$  for  $i = 1, 2$ , and  $\theta_i \equiv \arctg(y_i/x_i)$ , the total phase  $\Phi = \theta_1 + \theta_2$  decouples and the *three-dimensional* phase space motion is dictated by the equations

$$\begin{aligned} \dot{R} &= -2D \sin^2\left(\frac{\phi}{2}\right) R \\ \dot{r} &= -2D \cos^2\left(\frac{\phi}{2}\right) r \\ \dot{\phi} &= -2D \left(\frac{R^2 + r^2}{R^2 - r^2}\right) \sin \phi + [\omega(r_2) - \omega(r_1)], \end{aligned} \quad (4)$$

where  $\phi \equiv \theta_2 - \theta_1$ ,  $R \equiv r_1 + r_2$ , and  $r \equiv r_2 - r_1$ . Note that  $\phi$  represents the phase desynchronization between patches while  $r$  is the amplitude desynchronization.

### 2.1. Unstable system: Constant angular velocity

The simplest case, where the angular velocity is location independent,  $\omega(x, y) = \omega_0$ , and the migration rates are equal,  $D_1 = D_2 = D$ , allows for simple analysis. The problem is reduced to coupled *harmonic* oscillators. As Eq. (3) are now linear, the Lyapunov exponents of the *four-dimensional* system are given by the eigenvalues of the matrix

$$\begin{pmatrix} -D & \omega_0 & D & 0 \\ -\omega_0 & -D & 0 & D \\ D & 0 & -D & \omega_0 \\ 0 & D & -\omega_0 & -D \end{pmatrix}, \quad (5)$$

which are  $-2D \pm i\omega_0$  and  $\pm i\omega_0$ . The first two eigenvalues correspond to the relaxation of the *four-dimensional* dynamics to the homogenous (invariant) manifold, where  $x_1 = x_2$  and  $y_1 = y_2$ , and the Lyapunov exponent is  $-2D$ . After a transient time, the concentration on both patches is equal and the migration term becomes irrelevant. At this point the system is equivalent to a single patch system, the trajectories are bounded to the homogenous manifold, and the quantity  $R \equiv r_1 + r_2$  is conserved. The polar representation (4) is

$$\begin{aligned} \dot{R} &= -2D \sin^2\left(\frac{\phi}{2}\right) R \\ \dot{r} &= -2D \cos^2\left(\frac{\phi}{2}\right) r \\ \dot{\phi} &= -2D \left(\frac{R^2 + r^2}{R^2 - r^2}\right) \sin \phi. \end{aligned} \quad (6)$$

Clearly the phase desynchronization  $\phi$  (and consequently  $r$ ) approaches zero, leaving the invariant manifold  $R$  marginally stable,  $\dot{R} = 0$ .

Let us consider now the effect of noise. As explained above, for a system that admits a conserved quantity, like in the LV model, a single perturbation simply takes the system from one value of the conserved quantity ( $K$  for the LV case,  $R$  here). Noise, a series of uncorrelated perturbations, thus induces some sort of random walk in the conserved quantity space. As both  $K$  and  $R$  reflect the distance from the fixed point and are therefore bounded from below, the random motion leads to larger and larger values of the conserved parameter in the long run. In the LV case, this implies extinction when, due to the noise, one of the species reaches zero

density. The coupled oscillator model does not admit an intrinsic definition of extinction, but clearly if  $R$  grows unboundedly the system is in its “extinction phase”. Adding repulsion to the system (i.e.,  $\alpha > 0$ ) simply yields a rigid shift of the Lyapunov exponents by  $\alpha$ , and thus the marginally stable (LV like) system becomes unstable, Nicholson–Bailey like.

## 2.2. Spatial heterogeneity (SH)

The simplest stabilizing mechanism takes place when the environment is not homogenous, and the process parameters, like the growth rate of the prey, vary from one patch to another.

In fact, the observation that diffusive coupling between different spatial patches may stabilize otherwise unstable dynamics has been carried out in few disciplines independently. In ecology, (Murdoch and Oaten, 1975) suggested that dispersal between Lotka–Volterra patches with spatial variability may stabilize the coexistence fixed point. Subsequent studies (Crowley, 1981; Ives 1992, Murdoch et al., 1992; Taylor, 1998) consider the effects of multi-patch systems, parasitoid aggregation, difference in diffusion parameters, density different migration, and other complications. In chemistry, on the other hand, this stabilization is known as “oscillator death”, and was observed by Bar-Eli (1985) in the context of coupled chemical oscillators. That basic idea has been applied, since, to other diffusively coupled systems like neural oscillators (Kopell and Ermentrout, 1990) and calcium density fluctuations (Tsaneva-Atanasova et al., 2005). Mathematically speaking, the stabilizing effect of diffusive coupling between two sites on a single-species, extinction prone chaotic system has been considered by Gyllenberg et al. (1996).

Our toy model may be used very easily in order to demonstrate the fixed point stability for non-identical (different angular velocities,  $\omega_1 \neq \omega_2$ ) victim–exploiter patches.

$$\begin{aligned} \frac{\partial x_1}{\partial t} &= \omega_1 y_1 + D(x_2 - x_1) + \alpha x_1 \\ \frac{\partial y_1}{\partial t} &= -\omega_1 x_1 + D(y_2 - y_1) + \alpha y_1 \\ \frac{\partial x_2}{\partial t} &= \omega_2 y_2 + D(x_1 - x_2) + \alpha x_2 \\ \frac{\partial y_2}{\partial t} &= -\omega_2 x_2 + D(y_1 - y_2) + \alpha y_2. \end{aligned} \quad (7)$$

As this system is still linear, it may be diagonalized around the (only) fixed point at zero. When  $\alpha = 0$ , the Lyapunov exponent  $\Gamma$  for that fixed point turns out to be negative as long as  $|\delta| \equiv \omega_2 - \omega_1 \neq 0$  for any  $D$ , and approaches zero (marginal stability) if the dispersal is very small (no connection between oscillators), very large (single-oscillator limit) or if the system is homogenous ( $\delta \rightarrow 0$ ). The Lyapunov exponent is given by the equation in Box 1 and its typical behavior is illustrated in Fig. 2. Linearity implies that if the fixed point is stable it is also globally attractive.  $\Gamma$  parametric dependence is characterized by the following properties:

- Without loss of generality,  $\min(\omega_1, \omega_2)$  may be scaled to unity by rescaling the time. Thus the stability is determined by three parameters: migration rate, repulsion ( $\alpha$ ), and the desynchronization term  $\delta > 0$ .
- $\Gamma$  is a non-monotonic function of the migration rate; close to zero migration,  $\Gamma - \alpha$  vanishes linearly with  $D$ , while for large diffusion it decays like  $1/D$ . Maximum stability is obtained at the “optimal” dispersal  $D = \delta/2$ ; in which case  $\Gamma = \alpha - \delta/2$ .
- The only effect of  $\alpha$  is a rigid upward shift of  $\Gamma$ , as demonstrated in Fig. 2, where the dashed line indicates the border between the stable and unstable regime.

- For fixed migration an increase of  $\delta$  always helps to stabilize the system, but the effect saturates at  $\delta = 2D$ . Accordingly, for any  $\alpha$ , there is a critical diffusion below which the system turns to being unstable, independent of the level of heterogeneity.

Given that the system owed its stability to the migration between spatial patches, our toy model suggests an a priori estimate of the effect of spatial heterogeneity. The system will stabilize if  $D \sim \delta$  and  $D, \delta > \alpha$ . Experimentally,  $\alpha$  should be gathered from the single patch time to extinction, and if the decay is slow, and the populations oscillate a few times before extinction, one may acquire an estimate of  $\omega_1$  and  $\omega_2$  and find  $\delta$ . If it is also possible to attain an estimate for the per capita migration rate between patches, a reliable prediction about the importance of the SH mechanism may be made.

Even if the actual parameters cannot be recovered, our model allows for an a posteriori assessment of the role of spatial heterogeneity, based on local measurements, at least in some cases. The polar version of Eq. (7) is

$$\begin{aligned} \dot{R} &= \left[ \alpha - 2D \sin^2 \left( \frac{\phi}{2} \right) \right] R \\ \dot{r} &= \left[ \alpha - 2D \cos^2 \left( \frac{\phi}{2} \right) \right] r \\ \dot{\phi} &= -2D \left( \frac{R^2 + r^2}{R^2 - r^2} \right) \sin \phi + \delta. \end{aligned} \quad (8)$$

If  $r$  is negligible (e.g., when  $D \gg \delta$ ),  $\phi$  satisfies an equation for a forced pendulum,  $\phi = \arcsin(\delta/2D)$ . Thus, the SH route to stability is characterized, at least in this parameter regime, by a constant phase between the patches.

To get the flavor of all these consideration, we present in Fig. 3 the real space trajectories and the phase desynchronization time evolution for two coupled LV patches with spatial heterogeneity. One may realize the constant phase between patches that reflects the balance between the synchronizing effect of migration and the desynchronization induced by the heterogeneity.

To conclude, one should suspect that the SH mechanism plays an important role in the stabilization of a certain system if:

- An a priori assessment of the system parameters reveals that the characteristic migration rate is of order of the typical angular velocity difference between patches.
- Measurements of local population density show, at least on average, a constant phase between patches.

## 2.3. Environmental stochasticity (ES)

The above framework may also be used to consider the stabilizing effect of spatio-temporal environmental stochasticity (ES) (Reeve, 1988, 1990), at least in the large migration/weak desynchronization limit, as exemplified in Fig. 4. If on both patches the radial velocity takes the form  $\omega_i = \omega_0 + \zeta_i(t)$ , where  $i$  is the patch index and  $\zeta$  is a white noise that satisfies  $\langle \zeta(t)\zeta(t') \rangle = \gamma \delta(t - t')$  (here  $\delta$  is the Dirac delta function), the  $\phi$  variable in (7) obeys

$$\dot{\phi} = -2D \left( \frac{R^2 + r^2}{R^2 - r^2} \right) \sin \phi + \xi(t), \quad (9)$$

where  $\xi \equiv \zeta_2 - \zeta_1$  is also a Gaussian white noise. For small  $r$  this equation is equivalent to an overdamped noisy pendulum, and the desynchronization parameter  $\phi$  is distributed Gaussianly around zero, where its second moment satisfies  $\langle \phi^2 \rangle \sim \gamma/D$  (Gardiner, 2004).

The resulting motion on the invariant manifold satisfies

$$\dot{R} = (\alpha - \gamma) R \quad (10)$$

$$\Gamma = \alpha + \text{Re} \left[ -D + 1/2 \sqrt{4D^2 - 4\omega_1\delta + 2\sqrt{-(\delta + 2\omega_1)^2(-\delta^2 + 4D^2)} - 4\omega_1^2 - 2\delta^2} \right]$$

Box I.

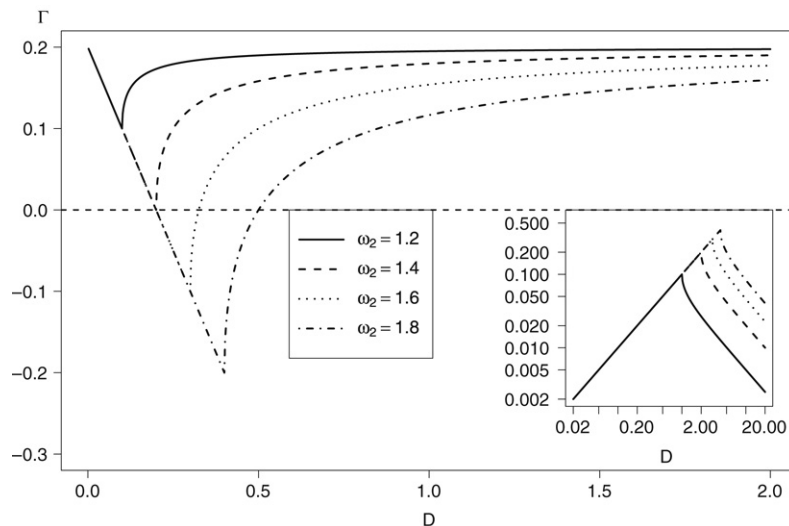


**Fig. 2.** The Lyapunov exponent of the system (7), plotted vs. the migration rate  $D$ . Parameters are  $\omega_1 = 1$  and  $\omega_2 = 1.2, 1.4, 1.6, 1.8$ , as indicated by the legend;  $\alpha = 0.2$ . Note that the system attains its maximal stability as  $D = \delta/2$ , as predicted. The inset shows the same lines for  $\alpha = 0$  in a log-log plot, to emphasize the asymptotic behavior  $D$  and  $1/D$ .

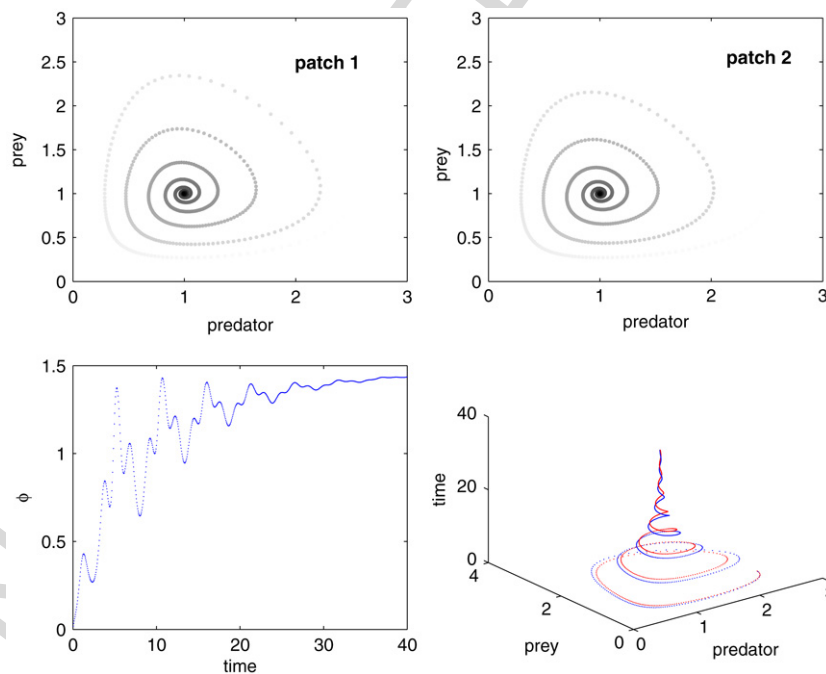


**Fig. 3.** The time evolution of two diffusively coupled Lotka-Volterra patches with spatial heterogeneity. In the absence of migration the inter-patch dynamics is governed by Eq. (1) with  $\mu = \sigma = \lambda = q$ , where  $q = 1.4$  on the first patch and  $q = 1$  on patch number 2. The fixed point is thus at (1, 1) for both patches, but the angular velocity, given (close the fixed point) by  $\omega = \sqrt{\mu\sigma}$ , is different. Both patches have the same initial conditions (predator density = 2.5, prey density = 1), and their phase space trajectories are illustrated in the upper two panels, where the gray level represents time (darker points = later time). The phase  $\phi$  between the two trajectories was initially zero and growth was due to the differences in angular velocities; in the presence of such phase differences, the migration becomes a stabilizing factor (see Fig. 1). In the lower left panel the desynchronization phase is shown to first increase, due to the spatial heterogeneity, then saturate because of the effect of migration. The overall result is a flow of the system toward the fixed point at (1, 1), as illustrated in the lower right panel. The migration rate was taken to be 0.2, and the results were obtained using forward Euler integration of the equations of motion with  $dt = 0.001$ . No noise was introduced and the trajectories are fully deterministic; in the presence of noise the population densities are distributed normally around the fixed point.

1 and the fixed point is stable if  $\mathcal{R} > \alpha$ . One should suspect that  
 2 the ES mechanism plays an important role in the stabilization of  
 3 certain system if:

- An a priori assessment of the system parameters reveals that  $\mathcal{R}$  is of order  $\alpha$ , i.e., the characteristic differences in oscillation rates of a single patch are larger than the “death rate”

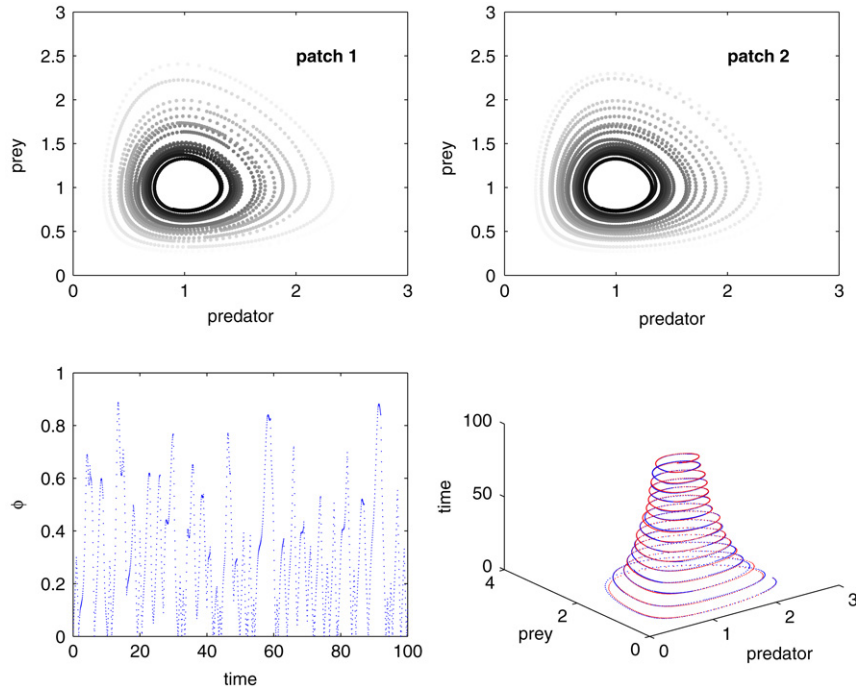


**Fig. 4.** The same as Fig. 3, but now  $q$  jumps randomly between 1.4 and 0.6. The convergence to the fixed point is much slower, and the (absolute value of the) desynchronization phase fails to saturate.

(the inverse extinction time) of such a patch.

• **A posteriori** measurements show correlations between the fluctuations of the desynchronization angle  $\phi$  and the fluctuating radius of oscillations  $R$ , but no connection between the amplitude difference  $r$  and the phase  $\phi$ . This is in sharp contrast with the ADAV mechanism considered below, where the  $r$  differences induce the desynchronization.

#### 2.4. Jansen instability (JI)

More than ten years ago, Jansen (Jansen, 1995; Jansen and de Roos, 2000; Jansen and Sigmund, 1998) put forward the idea of linearly unstable orbits of the Lotka–Volterra dynamics, i.e., orbits in the homogenous manifold for which the highest absolute value of an eigenvalue of the Floquet operator is larger than 1. This may occur only if the migration properties of the prey and the predator are different. In the case of equal diffusivities, the migration term factors out from the Floquet operator, and the stability properties of orbits lying in the invariant manifold are the same as their matching trajectories on a single patch (Abarbanel, 1995). However, Jansen pointed out that if one sets  $D_b = 0$  in the Lotka–Volterra equations, some orbits on the homogenous manifold may become unstable. This instability leads to a deviation of the trajectory from the homogenous manifold, and it turns out that the resulting flow is inward, leading to sustained oscillations of finite amplitude.

We have discussed Jansen’s stabilization mechanism in a different publication (Abta and Shnerb, 2007b); here we show how to incorporate this instability in our toy model. It turns out that the underlying mechanism relates to the dependence of the angular velocity along the orbit on the azimuthal angle, such that there are slow and fast regions along a single orbit. The angular velocity gradient creates a “shear” that tends to separate close points along the orbit, as in the CD region along the Lotka–Volterra orbit shown in Fig. 5. In the absence of migration to oppose that tendency, the system desynchronizes close to that part of the orbit and subsequently flows inward. See Fig. 6.

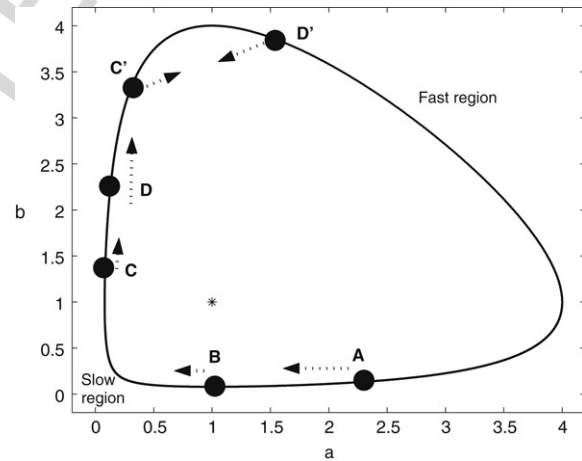


**Fig. 5.** An orbit of the LV dynamics ( $a$  is the predator density,  $b$  is the prey) and its fast and slow regions. For a two-patch system, if one patch is at point A along the orbit and the other patch at B, since the A patch is moving faster along the line it will get closer and closer to B during their flow toward the slow region. On the other hand, in the exit from the slow region the patch at D moves much faster than that at C, so they will desynchronize. As the predator density along this branch is almost constant, the only factor that may avoid desynchronization is the prey migration. In the absence of prey migration, the two patches reach the points C’ and D’, where the predator migration produces an inward flow.

We can mimic the Jansen mechanism using our toy model with  $\omega(\theta)$ . Specifically, the coupled oscillator model with

$$\begin{aligned} \frac{\partial x_1}{\partial t} &= \omega(\theta_1)y_1 + D_x(x_2 - x_1) & (11) \\ \frac{\partial y_1}{\partial t} &= -\omega(\theta_1)x_1 + D_y(y_2 - y_1) \\ \frac{\partial x_2}{\partial t} &= \omega(\theta_2)y_2 + D_x(x_1 - x_2) \\ \frac{\partial y_2}{\partial t} &= -\omega(\theta_2)x_2 + D_y(y_1 - y_2), \end{aligned}$$

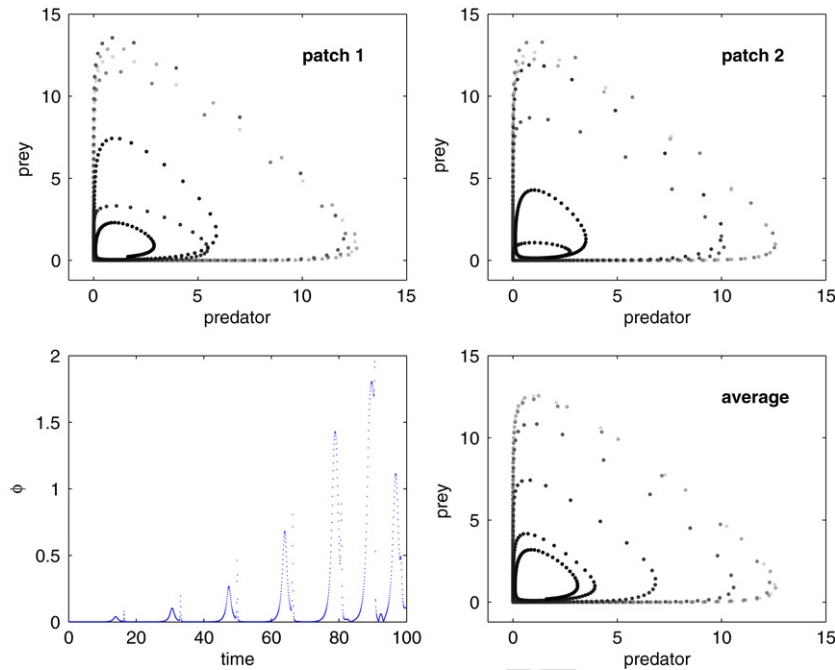


**Fig. 6.** The time evolution of two diffusively coupled, identical Lotka–Volterra patches with no prey migration (the predator migration rate is 1,  $\mu = \sigma = \lambda = 1$ ). The initial conditions are predator density = 12.5 on the first patch and 12.4 on the second patch, both with initial prey density 1. The phase space trajectories (darker points = later time) on each patch are shown on the upper panels, and the dynamics projected on the homogenous manifold (average populations) is graphed in the lower left panel. One can easily recognize that the inward flow happens during the multiplication stage of the prey, as suggested by the analysis following Fig. 5.

1 where  $D_x = D$ ,  $D_y = 0$  and  $\omega(\theta)$  may lead to the same type of  
 2 **Q10** instability.

3 To prove that this toy model actually yields Jansen’s instability,  
 4 we have used ( $i \in 1, 2$ )

$$5 \quad \dot{r}_i = \frac{(x_i \dot{x}_i + y_i \dot{y}_i)}{r_i} \quad \dot{\theta} = \frac{(x_i \dot{y}_i - y_i \dot{x}_i)}{r_i^2},$$

6 and

$$7 \quad r = r_2 - r_1 \quad R = r_2 + r_1 \quad \phi = \theta_2 - \theta_1 \quad \Phi = \theta_2 + \theta_1. \quad (12)$$

8 The flow in the invariant manifold ( $\phi = r = 0$ ) satisfies  $\hat{\Delta}$

$$9 \quad \dot{R} = 0 \quad (13)$$

$$10 \quad \dot{\Phi} = 2\omega(\Phi),$$

11 while the linearized equations for the desynchronization ampli-  
 12 tude  $r$  and the desynchronization angle  $\phi$  satisfy  $\hat{\Delta}$

$$13 \quad \frac{\partial}{\partial t} \begin{pmatrix} \phi \\ r \end{pmatrix} = \begin{pmatrix} 2 \frac{d\omega}{d\Phi} + 2D_x \sin^2(\Phi/2) & -\frac{2D_x}{R} \sin 2\Phi \\ 2D_x R \sin 2\Phi & -4D_x \cos^2(\Phi) \end{pmatrix} \begin{pmatrix} \phi \\ r \end{pmatrix}. \quad (14)$$

14 Using the Floquet operator technique to analyze the stability of  
 15 an orbit by integrating (14) along a close trajectory ( $R$  constant),  
 16 one finds the stability map presented in Fig. 7. Two unstable  
 17 regions appear, for large and small  $D_x$ . Note that in our toy model  
 18 the eigenvalues of the Floquet operator are  $R$  independent, so all  
 19 orbits share the same stability. In a realistic system, as in the LV  
 20 model, the dependence of  $\omega$  on  $\theta$  changes from one orbit to the  
 21 other, and a disk of stable orbits appears close to the coexistence  
 22 fixed point. One can easily show that, if  $\alpha = 0$ ,  $\dot{R}$  is a monotonically  
 23 decreasing quantity, vanishing only on the invariant manifold.  
 24 Accordingly, a limit-cycle like behavior is observed on the inner  
 25 surface of the unstable disk, as demonstrated in Abta and Shnerb  
 26 (2007b).

27 In the generic case of an unstable dynamics on a single patch,  
 28 i.e.,  $\alpha > 0$ , the situation is more complicated. First, the basic  
 29 analytical tool, the Floquet operator technique, fails in that case as

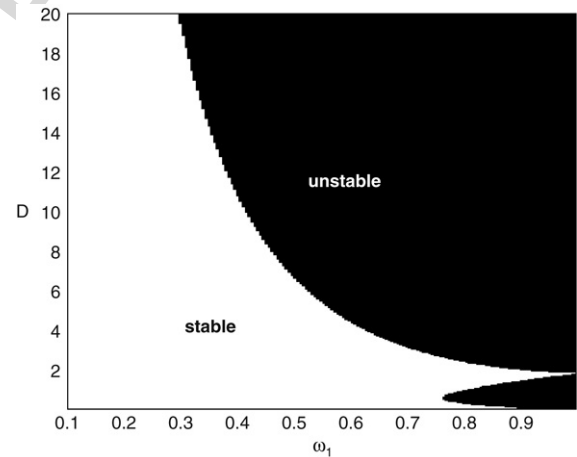


**Fig. 7.** Stability diagram in the  $\omega_1$ – $D_x$  plane for the Floquet operator for the coupled oscillator system described by Eq. (11) with  $D_y = 0$  and  $\omega = \omega_0 + \omega_1 \cos(\theta - \pi/4)$ .

the trajectories in the invariant manifold are not periodic. Second,  
 30  $\alpha$  appears also in the transfer matrix (14) in a non-trivial way.  
 31 However, assuming that the system is close to the marginal limit  
 32 (small  $\alpha$ ), one can characterize the systems in which stability is  
 33 archived via the Jansen mechanism:  
 34

35 **• A priori**, the system should allow for a large difference between  
 36 the migration rate of the two species involved, and in a  
 37 single patch the angular velocity around the coexistence point  
 38 strongly depends on the azimuthal angle.

39 **•** As explained in Abta and Shnerb (2007b), the instability  
 40 manifests itself when the azimuthal angular velocity gradient  
 41 is large, and is not balanced by the diffusion. This happens  
 42 when  $|\partial\omega/\partial\theta|$  takes its maximum along the trajectory at a point  
 43 where the fast migrating species gradient,  $|\partial x/\partial\theta|$ , is minimal.  
 44 The inward flow, thus, occurs at a specific point along the  
 45 trajectory, which may serve as a basic **a posteriori** identification  
 46 of the JI mechanism.

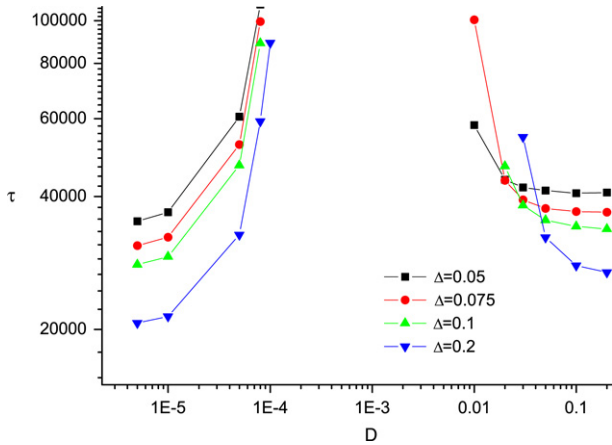


**Fig. 8.** Extinction times for the unstable, coupled oscillator cartoon of the Nicholson–Bailey model. Eq. (15) were integrated numerically (using Euler integration with  $\Delta t = 0.002$ ) for  $\alpha = 0.0001$  and  $\omega = \omega_0 + r/2$  for different noise amplitudes  $\Delta$  and diffusion constant  $D$ . The “extinction time” (extinction is declared when  $R$  becomes larger than some arbitrary value  $R_0$ ) is plotted for four different noise levels against the diffusion constant, and the transitions at high and low  $D$  are implicit. The lifetime of the system for large noise ( $\Delta = 0.1, 0.2$ , triangles) diverges beyond our computational abilities for  $D = 0.01$ . Note that, as  $D$  approaches infinity, the arguments (16)–(19) must fail, as for a single patch the extinction time is inversely proportional to the noise level; this explains the crossing of the lines in the right-hand side of the figure.

## 2.5. Amplitude dependent angular velocity (ADAV)

This mechanism has been presented by us recently in (Abta et al., 2007a). If the migration rate of the exploiter is close to that of the victim, this is the only known mechanism that yields stability in perfectly smooth environments, without spatial or spatio-temporal heterogeneity. Hence, it seems to be the only possible explanation for the numerical results showing sustainable predator–prey systems on perfectly homogenous spatial domains with equal diffusivities (Wilson et al., 1993; Bettelheim et al., 2000; Washenberger et al., 2006) and perhaps also for the experimentally calibrated numerics for bacterial systems (Kerr et al., 2002, 2006).

The mechanism requires migration, nonlinear dynamics and noise, and its route to desynchronization is the dependence of  $\omega$  on  $r$ . In terms of the toy model, and with additive noise, the Langevin equations take the form

$$\begin{aligned} \frac{\partial x_1}{\partial t} &= \alpha x_1 + \omega(x_1, y_1)y_1 + D(x_2 - x_1) + \eta_1(t) \\ \frac{\partial y_1}{\partial t} &= \alpha y_1 - \omega(x_1, y_1)x_1 + D(y_2 - y_1) + \eta_3(t) \\ \frac{\partial x_2}{\partial t} &= \alpha x_2 + \omega(x_2, y_2)y_2 + D(x_1 - x_2) + \eta_2(t) \\ \frac{\partial y_2}{\partial t} &= \alpha y_2 - \omega(x_2, y_2)x_2 + D(y_1 - y_2) + \eta_4(t), \end{aligned} \quad (15)$$

where  $\eta$  is a white noise that satisfies  $\langle \eta(t)\eta(t') \rangle = \Delta^2 \delta(t - t')$ . Assuming  $\omega(x_i, y_i) = \omega(r_i)$ , the system is invariant with respect to global rotation, and thus it reduces to the three-dimensional phase space:

$$\begin{aligned} \dot{R} &= (\alpha - 2D \sin^2(\phi/2)) R + \tilde{\eta}_R \\ \dot{r} &= (\alpha - 2D \cos^2(\phi/2)) r + \tilde{\eta}_r \\ \dot{\phi} &= -2D \left( \frac{R^2 + r^2}{R^2 - r^2} \right) \sin \phi + \omega(r_2) - \omega(r_1) + \left( \frac{\tilde{\eta}_1}{r_1} - \frac{\tilde{\eta}_2}{r_2} \right). \end{aligned} \quad (16)$$

Accordingly, close to the invariant manifold ( $r = \phi = 0$ ) the chance  $P(r)$  to find amplitude difference  $r$  is given by

$$P(r) \sim \exp[-(2D - \alpha)r^2/\Delta^2]. \quad (17)$$

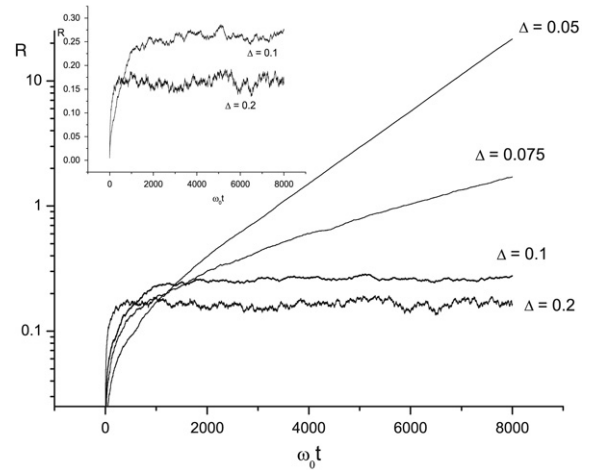


**Fig. 9.** Noise induced transition for the coupled oscillator cartoon of the Nicholson–Bailey model. Eq. (15) were integrated numerically (using Euler integration with  $\Delta t = 0.002$ ) with  $\alpha = 0.0001$ ,  $D = 0.01$  and  $\omega = \omega_0 + r/2$  for different noise amplitudes  $\Delta$ . The total distance  $R$  (averaged over 100 runs) is presented, in logarithmic scale, against time measured in units of  $\omega_0$ . Small noises are followed by exponential growth of the oscillation amplitude, as suggested by the deterministic part of (15). The larger the noise, the smaller the slope of this diverging line becomes. If the noise is large enough,  $R$  saturates at a finite value, as seen more clearly when the scale is not logarithmic (inset).

The  $\eta$  terms in the equation for  $\phi$  vanish at large  $R$ , and only the angular velocity gradient,  $\omega' \equiv d\omega/dr$ , determines the desynchronization:

$$\langle \phi^2 \rangle \sim \frac{\omega'(r)^2 \Delta^2}{D^2(2D - \alpha)^2}. \quad (18)$$

Consequently

$$\langle R^2 \rangle \sim \frac{\Delta^2}{D\langle \phi^2 \rangle - \alpha} = \frac{\Delta^2}{\omega'(r)^2 \Delta^2 / [D(2D - \alpha)^2] - \alpha}. \quad (19)$$

The system becomes unstable when either  $r^2$  or  $R^2$  diverge. The first criterion for stability comes from the amplitude synchronization parameter,  $2D > \alpha$ , so the diffusion should increase above some threshold value in order to prevent desynchronized extinction where the system acts as if made of two disconnected patches. If the migration rate is too large (i.e., if  $\alpha$  becomes larger than  $[\omega'(r)]^2 \Delta^2 / (2D - \alpha)^2 \sim \omega'^2 \Delta^2 / D^2$ ), the system synchronizes and the deterministic flow leads to synchronized extinction. Note that close to the low  $D$  transition the extinction rate grows with the noise, while close to the second transition, the increase of noise amplitude  $\Delta$  yields lower extinction rates, emphasizing the fact that the stability is noise induced. This feature is clearly seen in Fig. 9, where for small noise the oscillation amplitude grows exponentially in time while for large noise the oscillation stabilizes.

Eqs. (18) and (19) were derived under the assumption that the oscillation frequency depends linearly on the slope. If, on the other hand,  $\omega'$  is a non-uniform function of the amplitude, the oscillations will grow sublinearly (for the LV model) or exponentially (in NB case) with time, until they reach a phase space region where  $\partial\omega/\partial r$  is large enough. For an LV-like system this may lead to the appearance of a “soft” limit cycle – exponential convergence from the outside, random walk inside, similar to Jansen’s result. For a detailed comparison see Abta and Shnerb (2007b).

A simple illustration of the ADAV mechanism for the LV case is given in Fig. 10. Here, two patches are coupled by migration in the absence of noise, such that the homogenous manifold (where the two patches are synchronized) is stable. One notices

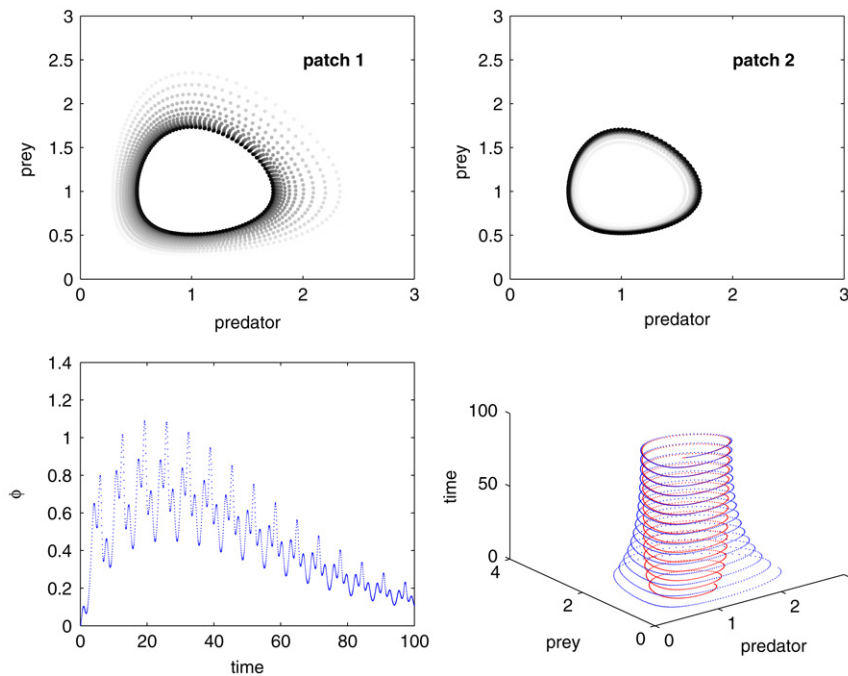


**Fig. 10.** The time evolution of two diffusively coupled, identical Lotka–Volterra patches with different initial conditions. In the absence of migration the dynamics on each site obeys Eq. (1) with  $\mu = \sigma = \lambda = 1$ . The initial conditions are predator density = 2.5 on the first patch and 1.5 on the second patch, both with initial prey density 1. In the absence of noise, migration makes the system homogenous after some characteristic time, leaving both patches synchronized; the desynchronization phase first grows due to the dependence of angular velocity on the oscillation amplitude, then decays as a result of migration (the parameters are migration rate = 0.02, Euler integration with  $dt = 0.001$ ). Note the decrease of the oscillation amplitude as a result of the initial difference; in the presence of noise (e.g., demographic stochasticity), differences between patches are generated continually, and the system is pushed toward the fixed point.

that, imposing different initial conditions between patches, the inward flow is much stronger during the synchronization process. Here, the system relaxed into a state of homogenous oscillations; in the presence of noise this process is iterated and may yield convergence to the fixed point.

- **A priori**, the relative importance of the ADAV mechanism may be calibrated using four parameters:  $\alpha$ ,  $D$ ,  $\Delta$  and  $d\omega/dr$ . In many cases it is difficult to attain a reliable estimate of these parameters (especially of  $\omega'(r)$ ) from the single patch dynamics. Thus, the identification of the ADAV mechanism should be based either on **a priori** disqualification of the other mechanisms or on **a posteriori** measurement.
- In particular, ADAV is characterized (a posteriori) by the correlation between the amplitude difference  $r$  and the phase desynchronization  $\theta$ , which is absent in the other mechanisms.

Finally, we remark that an additive noise is used here in order to model noise proportional to the size of the population, such as demographic stochasticity. This procedure may be justified using a self-consistency argument: we want to present a mechanism that stabilizes the population oscillations, such that the number of individuals in, say, the predator population, does not deviate strongly from its average value. If this is the case, the  $\mathcal{O}(\sqrt{N})$  noise amplitude does not change so much along the orbit, and the system “feels” constant (additive) noise.

### 3. Concluding remarks

Four different mechanisms that induce stability of population oscillations for metapopulations have been presented: a new mechanism that relies on the dependence of oscillation frequency on their amplitude, spatial heterogeneity, spatio-temporal environmental stochasticity, and Jansen’s mechanism based on the dependence of the angular velocity on the azimuthal angle.

It should be noted that the stability mechanisms presented here are applicable not only for the classic predator–prey systems but for any biological system that supports, locally, neutrally stable or unstable oscillations. In particular it may stabilize a “locally” unstable ecology of interspecific competition for common resources. Such a system may be described mathematically by the generalized Lotka–Volterra equations (Chesson, 2000); even if the theory predicts extinction, species diversity may be maintained on spatial domains.

In natural systems, in the laboratory, and in simulations, one may encounter population oscillations in the presence of a few of the above-mentioned factors, simultaneously. The task of the researcher is to make a distinction between them and identify the relevant, or most relevant, stabilizing mechanism. To accomplish this, a combination of the **a priori** and the **a posteriori** hints given above should be utilized. If some of the system parameters (like the dispersal rates, growth rates, or the level of stochasticity) may be subject to manipulation, the identification of the stability mechanism is much easier.

While we deal throughout this work only with continuous time systems, it seems that the basic insights presented here are valid also for the non-overlapping generations case. One should note, however, that even without an explicit noise term in the model, the chaotic (separating) features of a discrete map (like the NB one) yield an effective noise with varying strength along the trajectory. This may explain the appearance of stable (or nearly stable) trajectories in the multi-patch, **noise-free**, discrete NB dynamics (Adler, 1993). For this type of **map**, Hassell et al. (1991) show that **non-uniform** distribution of population on different patches may stabilize an otherwise unstable dynamics. It seems that the ADAV mechanism is responsible for that stabilization, where the noise here is “intrinsic”. We hope to present a more detailed study of this case elsewhere.

As pointed out by Jansen and Sigmund (1998), “all models of ecological communities are approximations: it is pointless to

burden them with too many contingencies and details. On the other hand, they would be of little help if they were not robust against the kind of perturbation and shocks to which a real ecosystem is ceaselessly exposed". The current accuracy of data on population oscillations and inter-specific interactions, both from field studies and from experiments, is, as far as we know, far below the level needed for an exact comparison with theoretical predictions about the oscillation phase portrait, like those predicted by the Lotka–Volterra model and its generalizations. Given that, the main insights from the available data are, first, the mere existence of these oscillations, and second, the identification of the underlying mechanism that limits the amplitude of these oscillations in noisy environments. As emphasized by the recent experiments, one may observe persistent oscillations or extinction, but it is difficult to compare the exact population dynamic with the predictions of the theory. Accordingly, the analysis of data on population cycles may be performed, as we have shown here, completely within the framework of the simple coupled oscillation model that allows all the suggested limiting processes within a transparent and general modeling scheme.

## Uncited references

Q11 Fig. 8.

## Acknowledgments

We acknowledge helpful discussions with David Kessler, Uwe Täuber, Gur Yaari, and Arkady Pikovsky. This work was supported by the Israeli Science Foundation (grant no. 281/03) and the EU 6th framework CO3 pathfinder.

## References

- Abarbanel, H.D.I., 1995. Analysis of Observed Chaotic Data. Springer, Berlin, p. 87.
- Abta, R., Schiffer, M., Shnerb, M.N., 2007a. Amplitude dependent frequency, desynchronization, and stabilization in noisy metapopulation. dynamics. Phys. Rev. Lett. 98, 098104.
- Abta, R., Shnerb, M.N., 2007b. Angular velocity variations and stability of spatially explicit prey–predator systems. Phys. Rev. E 75, 051914.
- Adler, F.R., 1993. Migration alone can produce persistence of host–parasitoid models. Amer. Nat. 141, 642–650.
- Allen, J.C., 1975. Mathematical models of species interactions in space and time. Amer. Nat. 109, 319–342.
- Bar-Eli, K., 1985. On the stability of coupled chemical oscillators. Physica D 14, 242–252.
- Bettelheim, E., Agam, O., Shnerb, N.M., 2000. "Quantum phase transitions" in classical nonequilibrium processes. Physica E 9, 600–608.
- Briggs, C.J., Hoopes, M.F., 2004. Stabilizing effects in spatial parasitoid host and predator prey models: A review. Theoret. Popul. Biol. 65, 299–315.
- Chesson, P., 2000. Mechanisms of maintenance of spatial diversity. Annu. Rev. Ecol. Syst. 31, 343–366.
- Crowley, P.H., 1981. Dispersal and the stability of predator prey interactions. Amer. Nat. 118, 673–701.
- Cuddington, K., 2001. The "balance of nature" metaphor and equilibrium in population ecology. Biology and Philosophy 16, 463–479.
- Ellner, S.P., McCauley, E., Kendall, B.E., Briggs, C.J., Hosseini, P.R., Wood, S.N., Janssen, A., Sabelis, M.W., Turchin, P., Nisbet, R.M., Murdoch, W.W., 2001. Habitat structure and population persistence in an experimental community. Nature 412, 538–543.
- Gardiner, C.W., 2004. Handbook of Stochastic Methods. Springer, Berlin.
- Gause, G.F., 1934. The Struggle for Existence. William and Wilkins, Baltimore.
- Gyllenberg, M., Osipov, A.V., Soderbacka, G., 1996. Bifurcation analysis of a metapopulation model with sources and sinks. J. Nonlinear Sci. 6, 329–366.
- Hassell, M.P., May, R.M., Pacala, S.W., Chesson, P.L., 1991. The persistence of host–parasitoid associations in patchy environments. I. A general criterion. Amer. Nat. 138, 568–583.
- Holyoak, M., Lawler, S.P., 1996. Persistence of an extinction-prone predator–prey interaction through metapopulation dynamics. Ecology 77, 1867–1879.
- Huffaker, C.B., 1958. Experimental studies on predation: Dispersion factors and predator prey oscillations. Hilgardia 27, 343–383.
- Jansen, V.A.A., 1995. Regulation of predator prey systems through spatial interactions: A possible solution to the paradox of enrichment. Oikos 74, 384–390.
- Jansen, V.A.A., de Roos, A.M., 2000. In: Dieckmann, U., Law, R., Metz, J.A.J. (Eds.), The Geometry of Ecological Interactions: Simplifying Spatial Complexity. Cambridge University Press, p. 183.
- Jansen, V.A.A., Sigmund, K., 1998. Shaken not stirred: On permanence in ecological communities. Theoret. Popul. Biol. 54, 195–201.
- Kerr, B., Neuhauser, C., Bohannan, B.J.M., Dean, A.M., 2006. Local migration promotes competitive restraint in a host–pathogen 'tragedy of the commons'. Nature 442, 75–78.
- Kerr, B., Riley, M.A., Feldman, M.W., Bohannan, B.J.M., 2002. Local dispersal promotes biodiversity in a real-life game of rock–paper–scissors. Nature 418, 171–174.
- Kirkup, B.C., Riley, M.A., 2004. Antibiotic-mediated antagonism leads to a bacterial game of rock–paper–scissors in vivo. Nature 428, 412–414.
- Kopell, N., Ermentrout, G.B., 1990. Oscillator death in systems of coupled neural oscillators. SIAM J. Appl. Math. 50, 125–146.
- Lotka, A.J., 1920. Analytical note on certain rhythmic relations in organic systems. Proc. Natl. Acad. Sci. USA 6, 410–415.
- Luckinbill, L.S., 1974. The effects of space and enrichment on a predator–prey system. Ecology 1142–1147.
- Murdoch, W.W., Briggs, C.J., Nisbet, R.M., Gurney, W.S.C., Stewart-Oaten, A., 1992. Aggregation and stability in metapopulation models. Amer. Nat. 140, 41–58.
- Murdoch, W.W., Oaten, A., 1975. Predation and population stability. Adv. Ecol. Res. 9, 1–131.
- Murray, J.D., 1993. Mathematical Biology. Springer-Verlag, New York.
- Nicholson, A.J., 1933. The balance of animal populations. J. Anim. Ecol. 2, 132–178.
- Nicholson, A.J., Bailey, V.A., 1935. The balance of animal populations. Proc. Zool. Soc. London Part I 3, 551–598.
- Pimentel, D., Nagel, W.P., Madden, J.L., 1963. Space–time structure of the environment and the survival of parasite–host systems. Amer. Nat. 97, 141–167.
- Reeve, J.D., 1988. Environmental variability, migration and persistence in host–parasitoid systems. Am. Nat. 132, 810–836.
- Reeve, J.D., 1990. Stability, variability, and persistence in host parasitoid systems. Ecology 71, 422–426.
- Redner, S., 2001. A Guide to First-Passage Processes. Cambridge University Press, Cambridge.
- Taylor, A.D., 1998. Environmental variability and the persistence of parasitoid host metapopulation models. Theo. Pop. Biol. 53, 98–107.
- Tsaneva-Atanasova, K., Yula, D.I., Sneyd, J., 2005. Calcium oscillations in a triplet of pancreatic acinar cells. Biophys. J. 88, 1535–1551.
- Volterra, V., 1931. Leçon sur la Théorie Mathématique de la Lutte pour le via. Gauthier-Villars, Paris.
- Washenberger, M.J., Mobilia, M., Täuber, U.C., 2006. Influence of local carrying capacity restrictions on stochastic predator–prey models. cond-mat/0606809.
- Wilson, W.G., de Roos, A.M., McCauley, E., 1993. Spatial instabilities within the diffusive Lotka–Volterra system: Individual-based simulation results. Theoret. Popul. Biol. 43, 91–127.